Lappeenranta University of Technology
Faculty of Technology
Department of Electrical Engineering

Bachelor's thesis

Silicon based 3D particle detectors in highly irradiative environments – A general view and simulation

Lappeenranta 25.11.2007

Author: Antti Penttinen 0244470
Instructor: M.Sc. Tanja Grönlund
Supervisor: Ph.D. Tuure Tuuva

TABLE OF CONTENTS

LIST OF SYMBOLS AND ABBREVIATIONS

α	Current damage factor
c	Constant for donor or acceptor removal
CCE	Charge collection efficiency
β	Introduction rate of defects
d	Thickness of a detector
ε	Dielectric constant
ε_0	Dielectric constant of vacuum
Φ	Radiation fluence
I_r	Leakage current
IEL	Ionizing energy loss
LHC	Large Hadron Collider
n	Donor-type doping
N_{eff}	Effective doping concentration
NIEL	Non-ionizing energy loss
p	Acceptor-type doping
SCR	Space-charge region
SLHC	Super Large Hardon Collider
U_{dep}	Depletion voltage
V	Volume
V_{fd}	Full depletion voltage

1. INTRODUCTION

Semiconductor detectors are used in many fields of applications for electrically detecting different atom- and sub atom-level particles, e.g. photons and neutrons. Most important of these fields in the near future include medical imaging using X-ray measurement, high-energy particle physics experiments and molecular biology research. These demand increasingly radiation tolerant and fast detectors to keep up with the requirements of the applications. The large hadron collider (LHC) in CERN is one of such application environments, detectors playing a crucial role in its functionality. After 2012 the device is to be upgraded to Super-LHC (SLHC) status, which increases the radiation to a level 10 times higher than the current level. High radiation exposure during long periods of operation inevitably deteriorate the properties of a detector, which is why new solutions are sought to have devices that can work adequately in such environments. Also very fast response rates will be needed in applications such as CERN linear collider (CLIC) where the measured phenomena occur much faster than the typical conventional planar detectors are able to process. These kinds of requirements are the main motivation for developing new detectors by the means of material, defect and device engineering.

Traditionally semiconductor detectors have been planar but recently different 3D structures, first proposed by Parker, Kenney and Segal (1997), have been in development. These new structures offer many advantages which are looked into in more detail in this paper. The most used material in detectors so far has been silicon since it offers reliable, cheap and fast devices. There also exist other viable material options for different applications but in this work the detectors are studied mainly from device engineering viewpoint. The main purpose of the work is to, at general level, discuss the main advances in detector research so far concentrating on 3D detectors and how they behave in high radiation environments. Also a basic 3D detector is simulated with Silvaco simulation software and the results are compared to a planar detector of same thickness to observe the differences of these two structure types. In addition to this, the depletion voltage of a 3D device is simulated with different irradiation doses.

2. SILICON DETECTORS

The main focus in this work is on silicon since it's the most extensively studied and used detector material. Other commonly studied semiconductor materials include several compounds such as GaAs, SiC and GaN. These are not as widely used, though, since their fabrication processes are more complex making the materials more expensive. Semiconductor detectors in general are based on the properties of a pn-junction, which consists of positively (acceptor) and negatively (donor) doped semiconductor sides. At the junction of these sides appears a space charge region (SCR), which is used for detecting different physical particles, such as photons, electrons and neutrons. When a particle arrives at the semiconductor, it induces free charge carriers which are then collected to electrodes by the electric field in SCR. By collecting the electrical charge, the original signal can be measured when its physical characteristics are known.

2.1 Requirements for future experiments

Radiation hardness is one of the key factors when considering semiconductor detectors for particle accelerators used in high energy physics experiments. Precise tracking of charged particles that decay quickly after collision is vital for the discovery of new particles. Therefore an LHC upgrade, called SLHC (Sadrozinski, 2005) is planned for the CERN collider to improve the statistics for important rare events. After the upgrade the detectors are expected to be exposed to total radiation fluences up to 1e16 neutrons/cm² with integrated particle charge even up to a few TeV during their operating life. It is crucial to maintain the charge collection efficiency (CCE) and control the build-up of radiation induced space charge. Also heavily temperature dependent charge trapping is a serious issue considering radiation hardness. Another result of the upgrade is the need for faster response time in order to avoid event pileup in readout.

2.2 Effects of radiation

During the long periods of operation semiconductor detectors collect large amount of particle radiation, which has multiple negative effects on their functionality. This aspect of detector research is discussed at more general level in this work, concentrating on the more well-known and -studied effects. Thus the focus is on

silicon. However, the general principles apply also to other semiconductors. Radiation damage in detectors can be roughly divided in two categories: bulk damage caused by non-ionizing energy loss (NIEL) and surface region damage caused by ionizing energy loss (IEL), which together alter the properties of the semiconductor and how the detector works.

2.2.1 Bulk defects

Bulk, i.e. lattice damage can appear due to following processes:

- displacement of lattice atoms by impurity particles;
- nuclear interactions;
- secondary processes involving defect clusters.

Displacement of a lattice atom leads to an interstitial, a foreign atom between regular lattice sites (locations of atoms in crystal structure), or a vacancy, an empty lattice site. These point defects create a single donor or acceptor state at deep level in the energy band gap of silicon. Especially the energy states near the middle of the band gap are hazardous for detectors, as they are most likely to be involved in thermal creation of electron-hole pairs. For a creation of a point defect to be possible, minimum recoil energy is required. In silicon this energy is 15 eV. High fluence particle radiation contains large amounts of high-energy charged or neutral particles. The elastic scattering of these particles provide enough energy to cause significant defects in detector material. Introduction of neutrons or protons will lead to a change of effective doping N_{eff} in semiconductor. Eventually it causes a type inversion, as shown in Figure 1. The changes in N_{eff} have direct effect on the resistivity of the undepleted bulk and V_{fd}, the voltage needed for full depletion, as discussed further in this chapter.

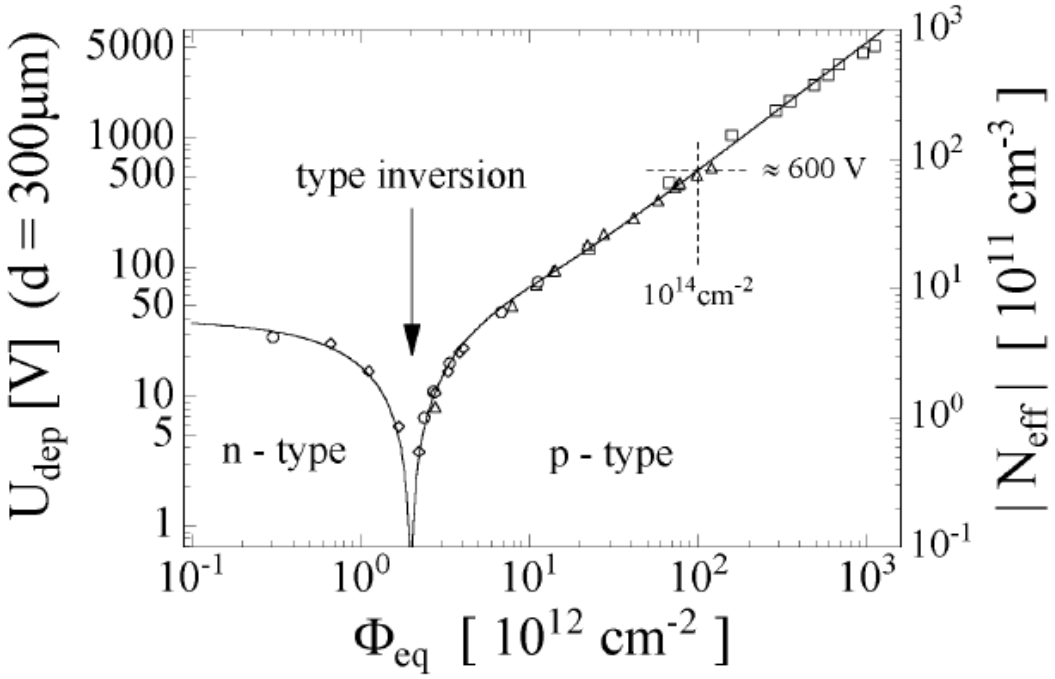

Figure 1. Example of measured changes in N_{eff} and U_{dep} (equal to V_{fd}) as function of radiation fluence (Wunstorf, et al., 1992).

Most of the primary defects mentioned here are not stable. Interstitials and vacancies are mobile at room temperature, which leads to partial annealing by an interstitial filling a vacancy or by diffusing out of the material surface. However, some defects may interact with another, forming defect complexes which are stable even at high temperatures (around 300 K) and have more significant effect on the electrical properties of the semiconductor. The exact formation method of complexes is only partially understood, however. Basically they are high concentration clusters of point defects and are typically the more common radiation-induced defect type. As described by Lutz (1999), defect complexes have some major effects on semiconductor:

- they act as recombination-generation centers, meaning that they can capture and emit charge carriers. In the space-charge region of a detector this leads to an increase of reverse-bias current;
- they act as trapping centers. Charge carriers are captured and emitted with a time delay, and in the space-charge region this trapping can reduce the efficiency of charge detection;
- they can change the charge density in SCR because of the change in N_{eff}, which increases the bias voltage requirement for making the detector operate

at maximum sensitivity.

These are the most important defect-induced changes in the operation of silicon detectors. Increased reverse-bias current means increased leakage current I_r, which is linearly related to the radiation fluence Φ according to the formula

$$I_r = \alpha \Phi V \,. \tag{1}$$

V is the depleted volume of the detector. The current damage factor α is dependent on temperature and the type and energy of irradiation. It can be determined by measurements for each situation. Charge carrier trapping delay is strongly dependent of the energy level depth of the trap. Very low level traps may release electrons or holes in short enough time for signal collection but generally trapping centers reduce the effective drift length of both charge carriers and thus deteriorate the detectors' charge collection efficiency, CCE.

The required voltage for full SCR depletion in a detector can be calculated from

$$V_{fd} = \frac{qN_{eff}d^2}{2\varepsilon\varepsilon_0}, \tag{2}$$

where d is the thickness of the detector, i.e. the distance between the electrodes of the detector, q the elementary charge and ε and ε_0 the dielectric constants of semiconductor and vacuum. On the other hand, the change of N_{eff} as a function of radiation fluence can be determined by

$$N_{eff}(\Phi) = N_{eff}(0)e^{-c\Phi} - \beta\Phi \,, \tag{3}$$

where $N_{eff}(0)$ is the initial effective doping concentration, c the constant of donor or acceptor removal and β the introduction rate of acceptor or donor-like defects (Casse, 2006). For simulation purposes, $N_{eff}(0)$ being small compared to fluence, this can be simplified as

$$N_{\text{eff}}(\Phi) = \beta\Phi \tag{4}$$

for p-type detectors. Whether the constants are for acceptors or donors depends on the type of defects. Figure 2 shows an example of radiation-induced deterioration in the CCE of a planar silicon detector. The deterioration is clearly visible as the radiation fluence grows.

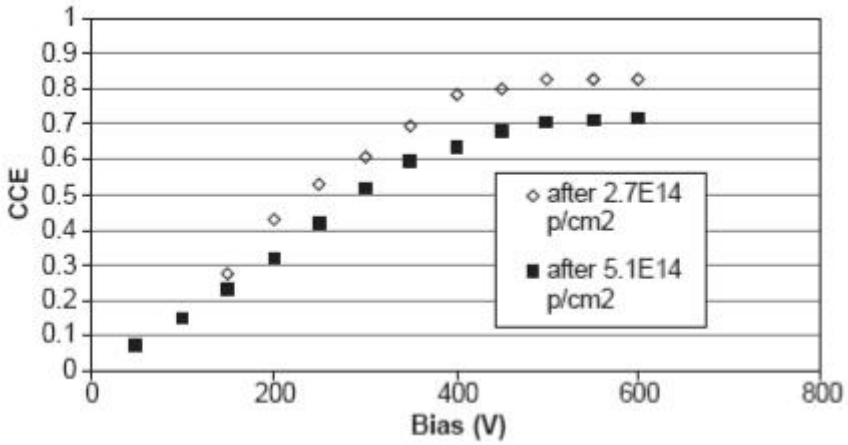

Figure 2. Charge collection efficiency as a function of bias voltage after different proton irradiation doses. Measurements were performed on oxygen enriched p-type silicon detectors. The plots are normalized to the value before irradiation. (Casse, 2004)

2.2.2 Surface defects

Radiation damage in the surface region of a detector, called oxide damage, consists mainly of damage in the insulator (typically SiO_2 is silicon devices) and in the insulator-semiconductor interface. The surface is highly irregular compared to the semiconductor bulk, which consists of nearly perfect single crystal. Therefore radiation damage to the material structure, i.e. nuclear interactions can be ignored. Instead, the oxide damage is caused by ionizing irradiation that supplies charge carriers to the surface area. By electron and hole capture as mechanism, these charges alter the charge states of defects that are already present in the oxide and the SiO_2/Si interface. The defects work as effective traps as the band gap of insulators is rather large, several eV, and the emission of captured charge carriers is difficult. Trapping of charges results in a build-up of charge which is seen as a shift in the flat-band voltage.

2.2.3 Reverse annealing

Reverse annealing is another phenomenon caused by irradiation that has to be considered when predicting the efficient operating lifetime of a detector. The effect was observed by Wunstorf, et al. (1992) while measuring the effective doping of irradiated silicon as a function of time. During long periods of annealing in room temperature the initial decrease of change in N_{eff} is followed by a new increase. This increasing change of N_{eff} takes place on the time scale of several months and is called reverse annealing. It is caused by the transformation of radiation-induced electrically inactive defect complexes into electrically active defects. The effect is accelerated by raising the temperature and slowed down by cooling (Lutz 1999). Usually cooling below 0°C is applied to minimize reverse annealing in detectors in high radiation environments, increasing their operating lifetime.

3. 3D DETECTOR

As mentioned in the introduction, this detector type was first suggested by Parker, et al. in 1997. A 3D detector can be considered as an evolved version of traditional planar detector. Its principle of operation is basically the same, but the new, different structural solution improves the detector properties. A typical 2D detector has its electrodes arranged in layer-like structure, as illustrated in Figure 3, which also shows the principal difference in electrode layout compared to 3D structure. Often the planar structure is simply called diode, which it principally is. The n+ and p+ electrodes are on both sides of the 300 µm thick Si bulk. When an ionizing particle enters the detector, it travels through the substrate generating charge carriers along its path. These electrons and holes are then collected for measurement to the readout electrode by carrier drift caused by an inter-electrode electric field. Reverse bias voltage is applied to the electrodes to deplete the bulk of free charge carriers. This dramatically increases the detector's ability to collect all charges induced by radiation.

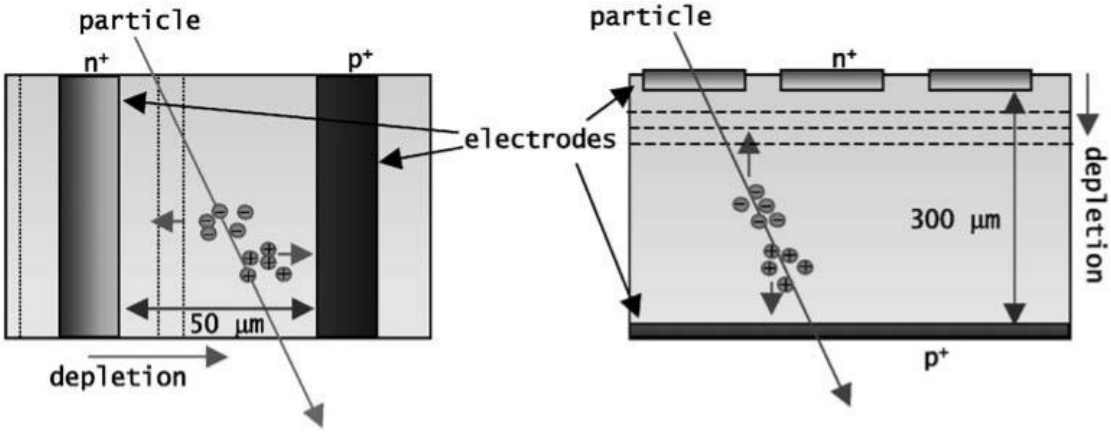

Figure 3. Cross section of a conventional 2D detector (right) and a 3D detector (left), where the same charge generated by an ionizing particle is collected in much shorter length. The dashed lines denote the growth of depleted area when a reverse bias is applied to the n+ electrode. The principle of radiation detection is same in both detector types. (Da Via, et al. 2003)

The different structure of 3D detector offers many advantages over 2D, which are especially useful in the applications previously discussed in this paper. Most notable of these is increased radiation hardness resulting from much shorter charge collection length, clearly seen in Figure 3, which results in significantly lower depletion voltage and faster charge collection time. The differences of these two device types are studied more closely in the following chapter. So far there have been successful simulations, fabrications and tests of different 3D detector structures. Also further studies and more detailed tests are under way to develop this detector type.

3.1 Operation and features

As explained, the basic principle of a 3D detector operation is similar to planar detectors. The radical difference is, however, that the electrodes are implemented as vertical columns inside the semiconductor substrate. Production-wise this structure is more complex to achieve but the advanced semiconductor manufacturing methods available these days have made it possible. The substrate is typically lightly doped n or p-type semiconductor and electrodes more heavily doped n+ and/or p+ -type columns which are arrayed in the way shown in Figure 4. The electrodes can be arranged in different patterns resulting in slightly varying detector performance.

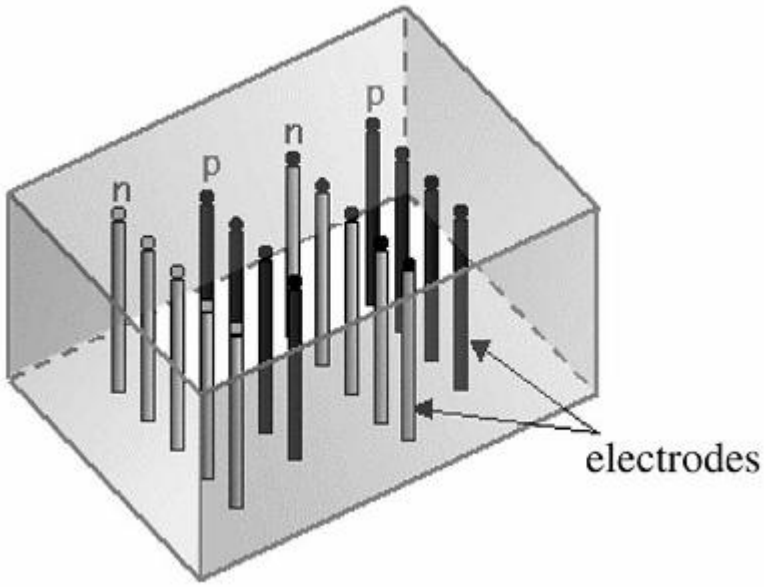

Figure 4. A schematic picture of a 3D semiconductor detector. n+ and p+ electrode columns penetrate through the bulk which can be n or p-type material. In this kind of structure the electrodes are typically 5-10 μm of diameter and at a distance of 30-100 μm from each other. (Da Via, et al. 2003)

In planar detectors the electrodes are at the surface and bottom of the structure and thus typically have a drift length of 300 μm, the thickness of the detector. 3D structure offers much shorter inter-electrode distance, as shown in Figure 3, which can be altered without changing the thickness of the detector, and charges can be collected notably faster. While planar detectors have charge collection time of 10-20 ns, a 3D detector can be as much as 10 times faster, having a collection time of 1-2 ns (Da Via, et al. 2003). Since the ionization track in 3D detector is parallel to the electrodes, all charges are almost at the same distance from these electrodes and arrive there simultaneously. This results in faster rise time of the signal improving the detector's speed even more. As a result of short distance between the electrodes this structure also needs to have only a small bias voltage, a few tens of volts, to completely deplete the bulk. A notable advantage of smaller required voltage is that breakdown protection becomes a subject of lesser concern.

This kind of electrode layout has also minor drawbacks, though. Firstly, the electrodes are so-called dead area which cannot be utilized for signal detection. This slightly reduces the effective area of the detector, depending on the size of the electrodes. Secondly, the region which is located in the middle between two electrodes of the

same type has lower electric field, which causes delay in collection of charge carriers that are generated in these regions. This effect can be avoided by over-biasing the device, however. (Fretwurst, et al., 2005)

The cylindrical shape of electrodes in 3D structure further enhances the operation. The geometry of the electric field is cylindrical, which results in higher average field in the drift path of the charges and increases the drift velocity and thus the detection speed. Another useful feature offered by 3D design is the possibility for drift time corrections to improve the accuracy of signal timing. This can be achieved by reading out from n+ and p+ electrodes simultaneously, as suggested by Kok, et al. (2006).

Another important intrinsic feature of the 3D structure is active edge. Traditional planar detectors usually suffer from a dead region near the physical edges. This undepleted area, which can't be used for signal detection, is at least as large as the thickness of the structure, typically ranging from 100 μm to 1mm (Kenney, et al., 2006). This region includes the space needed to keep the electric field away from the conducting saw-cut edges, which also can contain microcracks and other irregularities. When combined with the need for guard and voltage-dropping rings, the dead region can occupy even 14% of the total surface area (Kenney, Parker, Walckiers, 2001). While not being an absolute condition, in high-energy particle physics large detection area is desirable to save material. The particle detectors in colliders are arranged in multiple layers. As the particles travel through these layers, more active area allows better signal detection effectiveness. In 3D devices the dead area can be rather easily avoided by etching suitably doped trenches very close to the edges as shown in Figure 5. This results in much larger signal-sensitive area and minimizes the material usage, which in turn significantly reduces the loss of signal information caused by scattering and inelastic transactions. With current fabrication techniques it's become possible to reduce the insensitive border region down to 1-2 μm. However, this kind of active edge design is not limited to 3D devices exclusively, as studied more closely by Kenney, et al. (2001).

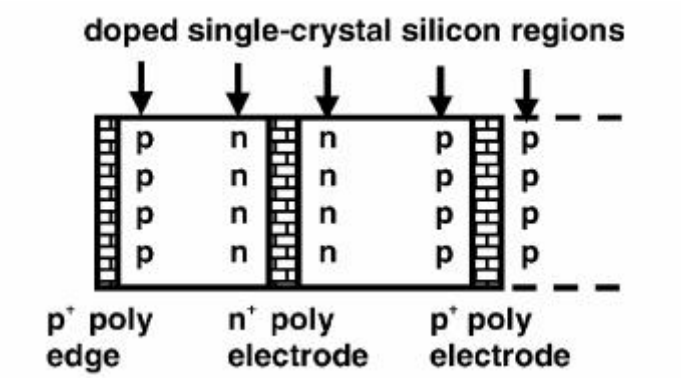

Figure 5. Schematic picture of an active edge detector. p+ dopant near the edges allow most of the device's area to be signal sensitive (Kenney, et al., 2006).

4. SIMULATION OF 3D DEVICE

In this work, Atlas device simulation software by Silvaco Data Systems Inc. is used for the characterization of simple 2D and 3D detector structures. Atlas is specifically designed for simulating electrical, optical and thermal behavior of semiconductor devices and is one of the most used simulation platforms in detector research. The motivation for simulating 3D detectors lies in easier and faster characterization of devices compared to actual measurements. Simulating saves time and costs which would otherwise be used for fabricating and measuring the detector. This holds especially for trivial measurements. For more complex situations however, simulation results cannot be taken as determining values but must be compared to measurements in order to have reliable results. Furthermore, for some simulations it is necessary to define certain parameters based on earlier measurements and studies. Since the main goal of simulations in this work is to study detectors at general level, very accurate modeling is not required however.

4.1 Simulation setup

In order to have better understanding of their differences, simulations are run with the same size for both 2D and 3D detectors. The height of the detectors is 300 µm and cross section area 70 x 70 μm^2. The n-type 2D structure has a 3 µm thick p-type layer on top of it and 0,5 µm thick aluminum electrodes are applied on top and bottom of the device. For 3D structure, a two-columnar electrode layout shown in Figure 6 is used. The electrode columns are sized 10 x 10 μm^2 and height of 270 µm is used because more mechanically durable detector is achieved if the electrodes don’t reach

all the way to the bottom of the structure (Fleta, et al., 2007). In the simulation electrodes are ¼ of their normal size since symmetry can be assumed in the situation, which allows reducing of the area and thus the amount of calculations needed. No guard rings or channel stoppers is used for simplicity of the situation. Normally the electrodes would be round as a result of the fabrication method. However, in simulation model squares are used instead because the grid for numerical calculation consists of triangles and as such it is easier to implement rectangular shapes. It would be possible to simulate spherical electrodes with some accuracy, but again it is not necessary to have a very detailed model in this case.

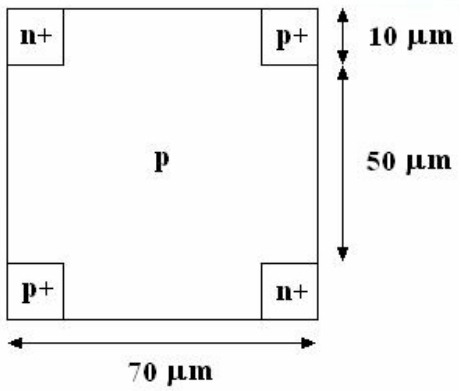

Figure 6. Cross section of a p-type 3D detector. The bulk doping p corresponds to the value of N_{eff} in each simulation case. Electrodes have doping concentration of $5x10^{18}$ cm^{-2}. P- and n-type areas are the opposite in n-type detector.

4.2 Depletion voltage in 2D and 3D structures

As discussed earlier, the voltage required for full depletion is strongly dependent on detector structure. From equation 2 it is possible to calculate theoretical values for V_{fd} in both structure types when they have the sizes mentioned in the previous paragraph. Values $2x10^{13}$ for the bulk doping concentration of both detectors and 11,8 for the dielectric constant of silicon are used. Table 1 contains the theoretical and simulated values for depletion voltage in each case. The 2D and 3D structures are simulated at several bias voltages to find the voltage at which the bulk is depleted. Depletion can be observed from the concentration of charge carriers, which reduces dramatically in depleted regions. Simulation results are presented in Figures 7 and 8, where the charge carrier concentrations are denoted as exponents normalized to the value of N_{eff} in the electrodes, which is $2x10^{13}$ in 2D and $5x10^{18}$ in 3D models.

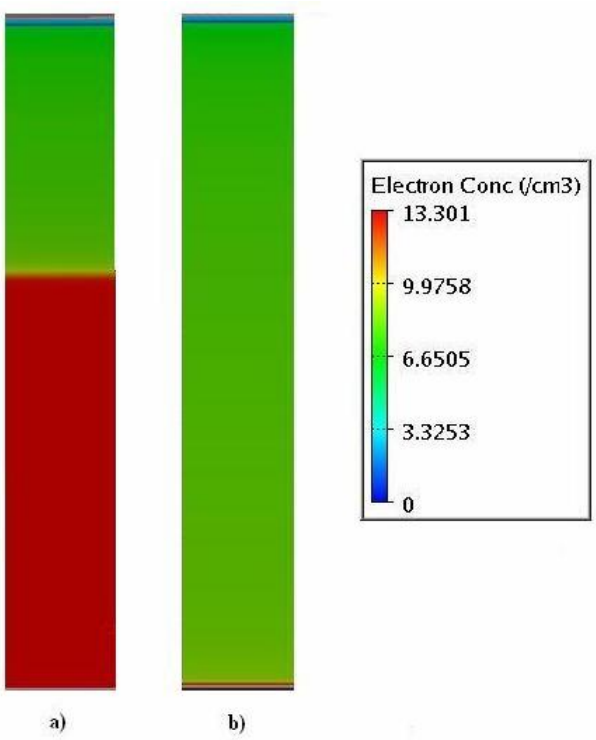

Figure 7. Bulk depletion of a n-type 2D detector at bias voltages of a) -200 V and b) -1400 V. Charge carrier concentration value $1x10^{13,301}$ equals to $N_{eff}=2x10^{13}$ in the electrodes.

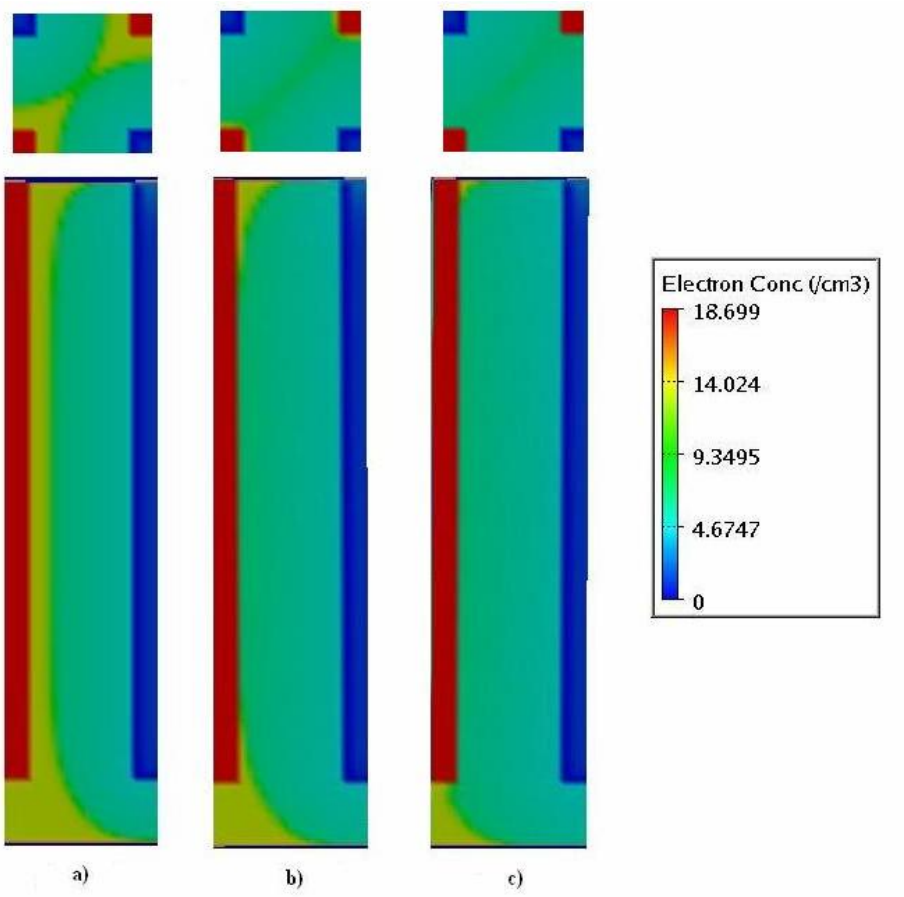

Figure 8. Bulk depletion of a n-type 3D detector at bias voltages of a) -40 V, b) -60 V and c) -100 V. Cross section images are taken from the middle of the structures.

Table 1. Theoretical and simulated values for V_{fd} in 2D and 3D detectors.

Detector type	**Distance between electrodes [µm]**	**Theoretical V_{fd} [V]**	**Simulated V_{fd} [V]**
2D	300	1380	1400
3D	50	38,5	60

4.3 Effect of irradiation on V_{fd} in 3D device

Detectors are exposed to large quantities of particle irradiation in their applications. The effect of irradiation doses can be observed by simulating the depletion voltage at different values for N_{eff}, since the doping concentration is dependent of radiation fluence according to equation 4. For this purpose a value for defect introduction rate is taken from earlier measurements for silicon detectors (Li, et al., 2004). Since accurate values for simulations are not necessary, assuming neutron radiation for this case also, a rounded value of 0,02 is used for the constant β. The radiation fluences

and their corresponding doping concentrations are presented in Table 2, which also has theoretical and simulated values for V_{fd}. Value 11,8 is used for the dielectric constant of silicon.

The depletion voltage can be simulated and observed by the same method as in the previous case. Figures 9 - 11 show simulated p-type 3D detectors with different bulk doping concentrations at bias voltages corresponding to theoretical V_{fd} and the voltage needed in simulations to fully deplete the bulk.

Table 2. Theoretical and simulated values for the V_{fd} of a p-type detector with different radiation fluences.

Φ [n/cm^2]	N_{eff} [cm^{-3}]	Theoretical V_{fd} [V]	Simulated V_{fd} [V]
1x10^{14}	2x10^{12}	3,9	8
1x10^{15}	2x10^{13}	38,5	60
1x10^{16}	2x10^{14}	385,2	500

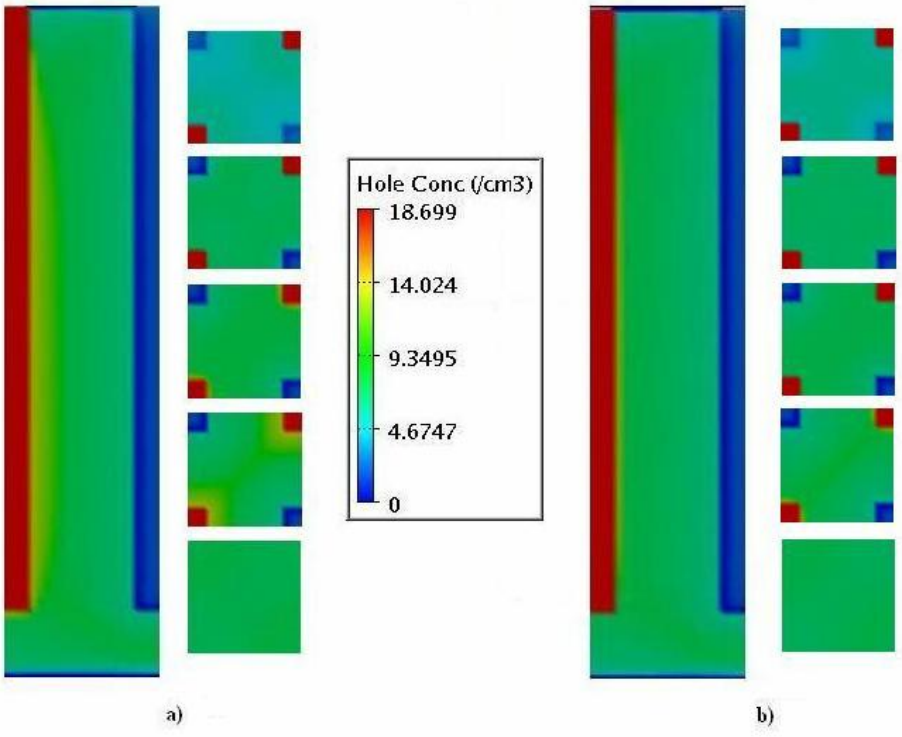

Figure 9. Bulk depletion of a p-type 3D detector with N_{eff}=2x10^{12} cm^{-2} at bias voltages of a) +4 V and b) +8 V. Cross sections are at distances 3, 15, 30, 150 and 285 µm from the top of the structures.

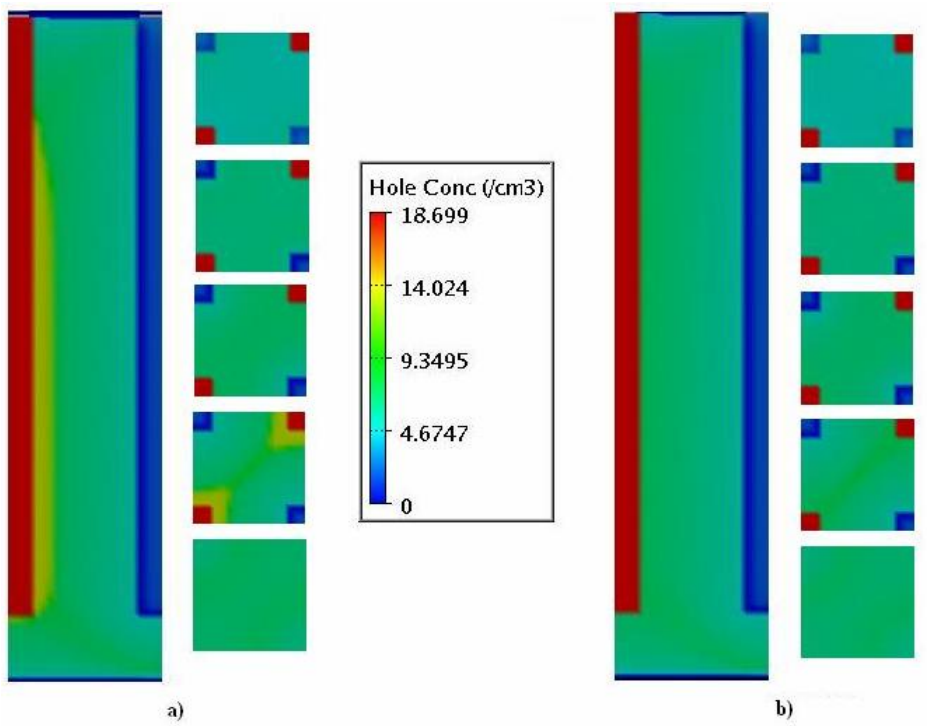

Figure 10. Bulk depletion of a p-type 3D detector with N_{eff}=2x10^{13} cm^{-2} at bias voltages of a) +40 V and b) +60 V.

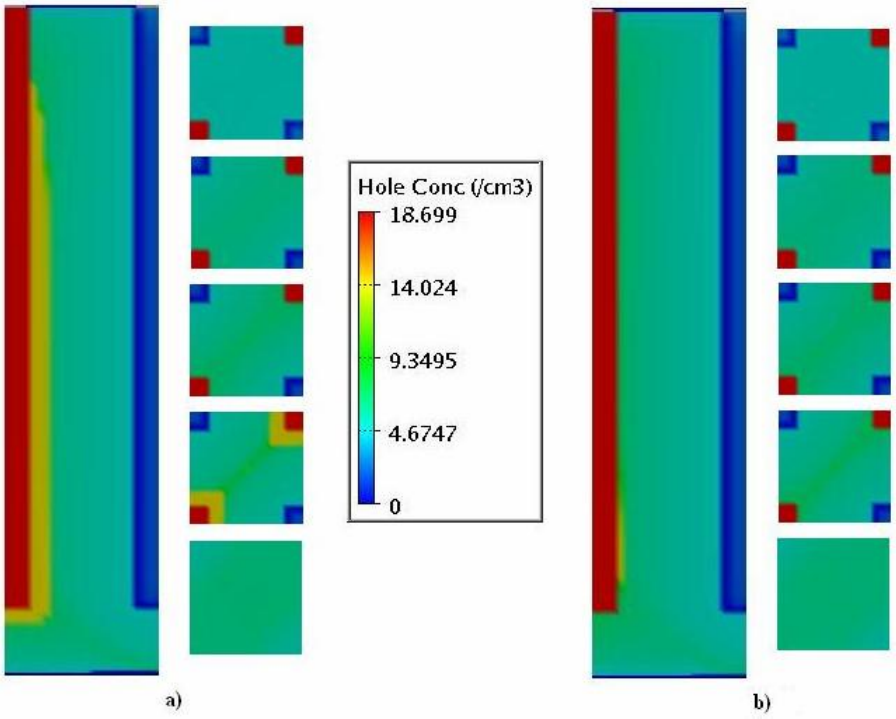

Figure 11. Bulk depletion of a p-type 3D detector with N_{eff}=2x10^{14} cm^{-2} at bias voltages of a) +400 V and b) +500 V.

4.4 Results

Since the simulations were done in rough voltage steps, the results are not very accurate. Despite that they give good enough approximation, especially in the case of 2D structure, which corresponds to theoretical results quite well. Also, the overall differences between depletion voltages of 2D and 3D detector structures and 3D structures under varying irradiation are clearly visible.

However, the simulated depletion voltages for 3D detectors are noticeably larger than theoretical calculations would suggest. All the 3D structures are still partially undepleted in their theoretical depletion voltages, which can be observed by the remnant charge carrier concentration near the n+ electrodes for n-type detector and p+ electrodes for p-type detectors (red columns in the figures). Moreover, the concentration is non-uniform; the n-type bulk depletes first from the center region and the p-type first from the upper part of the bulk. This can be partially attributed to the electrode layout and the behavior of the electric field in different biasing and doping. The main reason for larger depletion voltages is the so-called “zero-field” region (Fretwurst, et al. 2005) which is apparent in the middle area of detector cross section. The diagonal distance of the electrodes is larger than 50 µm, which is the length used in calculations. As such, the central parts remain with lower field strength in bias corresponding to the theoretical value. Another aspect to notice is that the original equations describing the electrical behavior of semiconductors are approximations in themselves and are derived using exclusively planar structures. Therefore it would seem that they are not very accurate for modeling actual 3D devices.

In addition to the simulations already described, a two-level radiation damage model introduced by Petasecca, et al. (2006) was to be used to further examine the effect of bulk defects on depletion voltage. However, there wasn’t a noticeable difference in results which contradicts theory and previous studies, which is why they aren’t included in this presentation. More detailed work concerning on how to implement different defect models into Silvaco simulation software is suggested.

5. CONCLUSION

A generic view of silicon detectors in high radiation applications was presented. It is possible to overcome the increasing radiation hardness requirements for particle

detectors by the means of device engineering. 3D structures can maintain much lower full depletion voltage than traditional planar devices making them good target for more extensive research and development. The most notable advantage of 3D structure is the short inter-electrode distance which offers fast charge collection and low depletion voltage.

3D simulations were performed on 2D and 3D detectors under different irradiation doses. The simulations of 3D structures give motivation for simulations being used in the research process in general. The results in this work show that numerical calculation methods are preferable over conventional mathematical equations when modeling three-dimensional devices because they don't describe 3D situations accurately enough. This would need further studies to prove it more extensively, though. Another motivation for simulations is that the behavior of charge carriers, the distribution of electric field etc. inside a detector can be observed easily without complicated measuring arrangements. So far there has been few publications concerning three-dimensional simulations of 3D devices, and the most commonly used software has been ISE-TCAD -platform. This caused trouble finding usable reference material for Silvaco-based simulations conducted in this work. However, the results give a general suggestion about the range of depletion voltage of 3D detectors which have similar structure to the one described here. To fully deplete a 3D detector under radiation fluences of magnitude of 10^{16} cm^{-2}, the bias voltage needs to be around 500 V. Also, over-biasing must be applied in order to get rid of "zero-regions" in middle parts of the detector. Required V_{fd} can be reduced by further improving device processing methods which allow smaller inter-electrode distance to be applied.

REFERENCES

Gasse, G., et al. 2004. First results on charge collection efficiency of heavily irradiated microstrip sensors fabricated on oxygenated p-type silicon. *Nuclear Instruments and Methods in Physics Research A*. **518**, pp. 340-342.

Casse, G. 2006. Prediction of the performances of finely segmented Si detector for tracking applications in future super-colliders after severe radiation damage. *Nuclear Instr. and Meth. A*. **566**, pp. 26-34.

Da Via, C., et al. 2003. Advances in silicon detectors for particle tracking in extreme radiation environments. *Nuclear Instr. and Meth. A*. **509**, pp. 86-91.

Eckert, S., et al. 2007. Signal and charge collection efficiency of a p-type STC 3D-detector irradiated to sLHC-fluences, readout with 40 MHz. *Nuclear Instr. and Meth. A*. **581**, pp. 322-325.

Fleta, C., et al. 2007. Simulation and test of 3D silicon radiation detectors. *Nuclear Instr. and Meth. A*. **579**, pp. 642-647.

Fretwurst, E. et al., 2005. Recent advancements in in the development of radiation hard semiconductor detectors for S-LHC. *Nuclear Instr. and Meth. A*. **552**, pp. 7-19.

Kenney, C., Parker, S.I., Walckiers, E. 2001. Results from 3-D silicon sensors with wall electrodes: near-cell-edge sensitivity measurements as a preview of active-edge sensors. *IEEE Transactions on Nuclear Science* **48**, pp. 2405-2410.

Kenney, C., et al. 2006. Active-edge planar radiation sensors. *Nuclear Instr. and Meth. A*. **565**, pp. 272-277.

Kok, A., et al. 2006. 3D detectors – state of the art. *Nuclear Instr. and Meth. A*. **560**, pp. 127-130.

Li, Z., et al. 2004. Radiation hardness of high resistivity magnetic czochralski silicon detectors after gamma, neutron, and proton radiations. *IEEE Trans. Nucl. Sci*. **51**, pp. 1901-1908.

Lutz, G. 1999. *Semiconductor radiation detectors*. Berlin Heidelberg: Springer-Verlag

Moll, M. 2006. Radiation tolerant semiconductor sensors for tracking detectors. *Nuclear Instr. and Meth. A.* **565**, pp. 202-211

Parker, S. I., Kenney, C., Segal, J. 1997. 3D – A proposed new architecture for solid-state radiation detectors. *Nuclear Instr. and Meth. A.* **395**, pp. 328-343.

Parker, S.I., Kenney, C. 2001 Performance of 3-D architecture silicon sensors after intense proton irradiation. *IEEE Trans. Nucl. Sci*. **48**, pp. 1629-1638.

Pellegrini, G., et al. 2003. Technology development of 3D detectors for medical imaging. *Nuclear Instr. and Meth. A.* **504**, pp. 149-153.

Petasecca, M., et al. 2006. Numerical simulation of radiation damage effects in p-type silicon detectors. *Nuclear Instr. and Meth. A.* **563**, pp. 192-195.

Sadrozinski, H. F.-W. 2005. Tracking detectors for the LHC upgrade. *Nuclear Instr. and Meth. A.* **552**, pp. 1-6.

Wunstorf, R., et al. 1992. Results on radiation hardness of silicon detectors up to neutron fluences of 10e15 n/cm^2. *Nuclear Instr. and Meth. A*. **325**, pp. 149-155.